Thick and high velocity crust in the Emeishan large igneous province, SW China: Evidence for crustal growth by magmatic underplating/intraplating

Yi-Gang Xu * and Bin He

Key Laboratory of Isotope Geochronology and Geochemistry, Guangzhou Institute of Geochemistry, Chinese Academy of Sciences, 510640 Wushan, Guangzhou, China

ABSTRACT

Geophysical, geological and petrologic data in SW China have been integrated in order to characterize magmatic unerplating associated with the late Permian Emeishan large igneous province (~260 Ma). Seismic reflection/refraction reveals a heterogeneous crustal structure, with high velocity layers/bodies in the upper crust (6.0-6.6 km/s), lower crust (7.1-7.8 km/s) and in the upper mantle (8.3-8.6 km/s). These seismically anomalous bodies are all confined in the inner zone of the pre-volcanic domal structure, but are generally absent in the intermediate and outer zones. There is a decreasing trend in crustal thickness from the inner zone (>60 km, with a ~20 km thick high velocity lower crust - HVLC) via the intermediate zone (~45 km) to the outer zone (<40 km). Since the domal uplift immediately preceding eruption of the Emeishan basalts is unambiguously related to a mantle plume, such a configuration highlights a genetic relationship between the formation of the high velocity crust and the mantle plume that led to the eruption of the Emeishan basalts. It is proposed that the HVLC may have resulted from magmatic underplating associated with the Emeishan volcanism, whereby the fast mantle represents the residues left after extensive melt extraction from the plume head. Magmatic underplating can also account for the prolonged crustal uplift which formed the Chuandian "old land" in SW China. Petrologic modeling further suggests that the HVLC may represent fractionated cumulates from picritic melts and the Emeishan basalts represent residual melts after polybaric fractionations. This relationship allows a re-estimate of the volume of Emeishan magmas, which is as much as 3.8 x 10^6 km^3, typical of plume-generated LIPs in the world.

Keywords: Mantle plumes, uplift, underplating, petrologic modeling, Emeishan

INTRODUCTION

Magmatic underplating is an important feature of large igneous provinces (LIPs). On the basis of basaltic compositions and mantle melts, Cox (1980, 1993) suggested that ponding and polybaric fractionation of primary picritic magmas at the base of crust may be an important process in the generation of continental flood basalts, and magmatic underplating is a potentially large contribution to the crustal accretion. This hypothesis has received supporting evidence in geophysical, geological and geochemical/petrologic observations for

* Corresponding author: E-mail: yigangxu@gig.ac.cn

over 20 years.

First, there is a growing body of seismic data that allows imaging of the crust-mantle structure of hotspots (e.g., Watts and ten Brink, 1989; Caress et al., 1995), of volcanic rifted margins (e.g., White et al., 1987; 1989; Barton and White, 1995; Bauer et al., 2000; Menzies et al., 2002) and of oceanic plateaus (e.g., Furumoto et al., 1990; Mauffret and Leroy, 1997). Seismic data consistently indicate crustal thickening and the existence of high-velocity layers at the base of the crust in LIPs. The thickness of these layers ranges from a few to more than 20 km, and their seismic velocities are intermediate between those of the mantle (>8 km/s) and those typical of the lower crust (<7 km/s). These high velocity layers are commonly interpreted as results of magmatic underplating (Kelemen and Holbrook, 1995; Farnetani et al., 1996; Trumbull et al., 2002).

Second, subsidence and exhumation history in basins of volcanic rifted margins and permnant uplift in the continental LIPs, are surface manifestation of the geologic processes in depth. As the lithosphere is thinned by uniform stretching, rifts and basins subside to maintain isostatic equilibrium, while in volcanic rifted margins this subsidence is counterbalanced by uplift resulting from the addition of new igneous material to the crust (White et al., 1987; 1989). Many basins in North Atlantic volcanic rifted margins underwent permanent uplift of several hundred meters, which was likely caused by magmatic underplating (Sanders et al., in press). After having studied drainage patterns of three continental LIPs, Cox (1989) suggested topographic doming associated with plume activity can be preserved after ~200 Myr, and crustal thickening by magmatic underplating is the most likely cause for the persistence of such features. Although the work by Cox (1989) on the Deccan traps receives some criticism (Sheth, this volume), the link between underplating and persistant uplift remains valid.

Finally, petrologic modeling provides supporting evidence for the hypothesis of magmatic underplating beneath the LIPs. On the basis of thermal and petrophysical modeling, Furlong and Fountain (1986) suggested that more than 10 km thick underplating layer (Vp=7.0-7.8 km/s) has been added to base of the continental crust. Farnetani et al (1996) used the petrological code MELTS to model the compositional evolution of primary picritic magmas, assuming that crystal fractionation is the dominant mechanism through which picritic liquids evolve toward a basaltic composition. They argued that high-velocity layers (7.4-7.9 km/s) detected at the base of the crust beneath oceanic and hotspot tracks may represent fractionated cumulates from picritic magmas.

Magmatic underplating is therefore an integral part of volcanism and can be constrained in three independent ways, namely, geophysical, geologic and petrologic approaches. Although individual approach has been used to characterize magmatic underplating in LIPs, so far, no multidisciplinary integration has been performed in a single continental LIP. The late Permian Emeishan flood basalt in SW China is ideal for such an exercise, because the evidence from all three aspects is present. (1) A lot of geophysical experiments (e.g., deep seismic sounding, seismic tomography and gravity survey) have been performed in this region since 1980's, thus providing insights into the crust-mantle structure. (2) Sedimentary evidence has been preserved for the crustal uplift before and after the Emeishan volcanism, which is likely related to deep processes (He et al., 2003, 2006; Xu et al., 2004); and (3) the Emeishan basalts and coeval layered mafic and ultramafic intrusions are well exposed in this region and have stimulated many petrologic and geochemical analyses (Chung and Jahn,

1995; Xu et al., 2001; Zhou et al., 2002, 2005; Zhong et al., 2004). This makes it possible to determine the nature of cumulate products left in the depth by fractionation of the Emeishan basalts.

In this contribution, we review geophysical data available in this area and highlight main characteristics of crust and mantle structure in the Emeishan LIP. In particular, we view the spatial variation in crustal thickness in relation to the domal structure defined by sedimentary data (He et al., 2003), which has been interpreted as plume-induced uplift. We attribute the unusually thick, and high velocity crust in the central part of the Emeishan LIP to magmatic underplating and/or intraplating. The nature of underplated materials is constrained by relating petrologic modeling results to observed seismic velocity.

GEOLOGICAL BACKGROUND AND PREVIOUS STUDIES

The Late Permian Emeishan basalts are erosional remnants of the voluminous mafic volcanic successions occurring in western margin of the Yangtze Craton, SW China. They are exposed in a rhombic area of 250 000 km^2 (Xu et al., 2001) bounded by the Longmenshan thrust fault in the northwest and the Ailaoshan-Red River slip fault in the southwest (Fig. 1). However, some basalts and mafic complexes exposed in the Simao basin, northern Vietnam (west of the Ailaoshan fault), and in Qiangtang terrain (northwest of the Longmenshan fault) make possible an extension of the Emeishan LIP (Chung et al., 1998; Xiao et al., 2003; Hanski et al., 2004). The Red-River fault is also considered as a suture zone along which the Yangtze craton was subducted by at least 150 km underneath the Sanjiang tectonic zone (Liu et al., 1998). Therefore, besides translational disruption by the Red-River fault, the Emeishan LIP was also affected by reworking during Mesozoic closure of Tethys Ocean and the Cenozoic collision between the Indian and Asian continents.

The Emeishan basalt uncomfortably overlies the late Middle Permian carbonate Formation (i.e., the Maokou limestone) and are in turn covered by the uppermost Permian in the east and west, and the upper Triassic sediments in the central part. A number of observations indicate that the central part of the Emeishan LIP has experienced uplift: (1) Most of flood basalts were eroded away in the inner zone except remnant in few localities. Most of remnant flood basalts are distributed in the intermediate zone (Fig. 1); (2) Moderate and high-grade metamorphic Mesoproterozoic Kangding complex, Neoproterozoic spilite-keratophyre sequence with green-schist facies metamorphism and epimetamorphic sedimentary rock sequence are exposed in the inner zone (Pre-Cambrian metamorphic crystalline basement is exposed). However, mainly Paleozoic sedimentary sequences are exposed in the intermediate zone. (3) Numerous layered mafic intrusions and ring felsic complexes are exposed only in the Central Emeishan LIP. To further characterize this area, He et al. (2003) correlated and compared the biostratigraphic unit of the Maokou Formation and showed a systematic thinning of the strata beneath the Emeishan basalts. The surface of thinned carbonates is an unconformity, having karst paleotopography and local basal conglomerates, the clasts of which were derived from the uppermost Maokou Formation. This suggests that stratigraphic thinning likely resulted from differential erosion due to regional uplift. Isopachs of the Maokou Formation further delineate a circular uplifted area (He et al., 2003), very similar to the crustal doming above an upwelling mantle plume

predicted by laboratory experiments (Campbell and Griffiths, 1990) and by numerical simulations (Farnetani and Richards, 1994). Pre-volcanic crustal doming in the Emeishan LIP led to a new division of the province, i.e., inner, intermediate and outer zones (Fig. 1), which have different extents of erosion of the Maokou Formation (He et al., 2003).

The Emeishan flood volcanism succession comprises predominantly basaltic flows and pyroclastic deposits, with minor amounts of picrites and basaltic andesites, with a total thickness ranging from several hundred meters up to 5 km (Xu et al., 2001). The Emeishan basalts have been divided into two major magma-types: high-Ti (Ti/Y>500) and low-Ti (Ti/Y<500) basalts (Xu et al., 2001). Data compilation reveals a systematic change in basalt type from the inner to intermediate zones (Xu et al., 2004). In general, the domed region comprises *thick* (2000 – 5000 m) sequences of dominant low-Ti volcanic rocks and subordinate picrites (Chung and Jahn, 1995), high-Ti and alkaline lavas (Xu et al., 2001, 2003; Xiao et al., 2003). In contrast, *thin* sequences (<500 m) of high-Ti volcanic rocks mainly occur on the periphery of the domal structure. It has been shown that the high-Ti and low-Ti lavas require very different mantle conditions (Xu et al., 2001). As such, this spatial variation reflects the thermal gradient of the mantle from which the Emeishan basalts were derived (Xu et al., 2004).

GEOPHYSICAL EVIDENCE FOR A THICK AND HETEROGENEOUS CRUST IN THE EMEISHAN LIP

Geophysical investigation has been carried out in this region since 1980's with the purpose of mineral explorations and of characterizing the crust-mantle structure under the Emeishan LIP (Tan, 1987; Zhang et al., 1988; Teng, 1994). The experiments include six deep seismic sounding (DSS) profiles (Xiong et al., 1986; Cui et al., 1987; Yan et al., 1986; Tan, 1987), several seismic tomography (Zhang and Ma, 1985; Sun et al., 1991; Liu et al., 2000), besides gravity and magnetic measurements (Liu et al., 1987; Teng, 1994). Such data are of critical importance in understanding the crust-mantle structure in this area. Unfortunately, most of these data were published in Chinese literature that is not accessible to foreign researchers. In this section, the main features of these geophysical data will be summarized with special attention to spatial variation of crust-mantle structure in relation to the domal structure.

Deep Seismic Sounding (DSS)

General description of methods

During long-range seismic wide-angle profile refraction/reflection investigations, large (1-38t) shots fired in deep (20-30 m) holes were used to probe deeply and obtain clear seismic arrivals from the crust and upper mantle. 196 sets of analog magnetic tape recorders (GPS, France; 7030G, Germany; DZSM-1, China) were employed along the profiles to record timing and shot-instant pulses (detector distance: 1.5-3 km). 4-8 shots were fired for each profile. In the field, a split spread configuration was used for each shot point, whereby seismographs were deployed on both or one side of each shot point. Altogether, up to 240 recording sites were occupied along the profiles (two deployments of 120 instruments) by the

portable FM cassette-tape recording seismographs. The usability of the seismic data was 86.4-73.2%. Seismic phases were identified by their kinematic and dynamic characteristics on the record section graphs.

In order to build a reasonable initial crust model, different methods (e.g., the common depth point, t^2-x^2, time term and different time-distance methods) were used. Both forward and inverse velocity travel-time modeling were employed in establishing the crustal models. Details of the experiments and data treatment can be found in Teng (1994). Here, we briefly summarize the main features of four DSS profiles, which traverse different parts of the Emeishan LIP (Fig. 1).

Lijiang-Zhehai Profile (A-A')

This E-W trending profile is 350-km long and runs over the inner zone of the Emeishan LIP (Fig. 2a). It is centered on the Panzhihua site – the second largest V-Ti magmatic ore deposit in the world. The crust under this profile can be divided into three layers. The upper crust is ~25 km thick with Vp ranging from 4.0 to 6.6 km/s. The velocity of the uppermost crust (<5 km) in the middle part of the profile (5.8–6.0 km/s) is higher than those in western and eastern ends (4.2-5.5 km/s). This might indicate the presence of mafic sills and intrusions in the center part of the Emeishan LIP. The velocity increases to 6.3-6.6 km/s at the lower part of the upper crust, significantly higher than the average velocity of the continental upper crust (< 6 km/s; Rudnick and Jackson, 1995). It then decreases to 5.6-6.0 km/s in the depth range of 26-40 km (middle crust). The lower crust extends from 40 to 55 km and is characterized by Vp of 6.5 to 6.8 km/s. Higher velocity (6.8-7.0 km/s) has been observed locally (Tan, 1987). This layer is sitting above a layer of 7.6-7.9 km/s. Similar velocity layer is also detected in the Lijiang-Xinshi profile (see next sections). However, higher velocity (>8.0 km/s) observed in the Lijiang-Xinshi profile is not detected along this profile. While the interpretation of the layer of 7.6-7.9 km/s remains uncertain, the crust beneath the inner zone is at least 55 km, which is thicker compared to those in other part of the Yangtze Craton (~40 km).

Lijiang-Xinshi Profile (B-B')

This NE-trending profile is 407-km long and runs across the inner zone and intermediate zone of the Emeishan LIP. The gross crustal structure along this profile is shown in Fig. 2a. The most salient feature is that the crust is segregated by Xiaojiang fault, Anninghe fault and Jinhe fault which cut through the lower crust and reach the upper mantle. The crustal thickness under the center of the profile could be >70 km if the layer of 7.6-7.8 km/s is taken as a part of the lower crust. The high-velocity rock body (~6.0 km/s) near the surface in the center part of the Emeishan LIP is probably related to mafic sills and intrusions.

Simao-Malong Profile (C-C')

This profile is situated outside of the Emeishan LIP and crosses the Red-River fault (Fig. 1). The crustal thickness in this region ranges from 37 to 45 km (Fig. 2c), significantly lower than those in the inner zone of the Emeishan LIP. Another salient feature is that the layer with velocity (7.6-7.8 km/) intermediate between crust and mantle is not present under this region. P wave velocity of the upper mantle is 8.06-8.10 km/s.

Heishui-Wulong Profile (D-D')

This profile is located in the northern part of the outer zone of the Emeishan LIP. The crustal thickness in this region ranges from 40 to 45 km (Fig. 4d). A thin (<5 km) layer with Vp of 7.1-7.4 km/s is detected at the middle of the profile.

Seismic Tomography

Seismic tomography along the Lijiang-Zhehai profile (same as the DSS profile A-A') is reproduced in Fig. 3. The best horizontal resolution for this velocity image is 20-30 km and the best vertical resolution is 10-15 km in the crust and about 30 km in the upper mantle (Liu et al., 2000). Three main features are noted from Fig. 3.

(a) A heterogeneous velocity structure is observed in both vertical and horizontal directions. Vertically, continuous and discontinuous alternating high and low-velocity strip-shaped zones are observed at different depths. Horizontally, high- and low-velocity strips are obviously divided into several sections and the strongest heterogeneity of the crustal structure is near the central part of the Emeishan LIP, in which 6.0 km/s is found at the depth of 5 km. A high-velocity (6.1-6.4 km/s) lens-shaped body of 60 km long and 10 km thick is present in the upper crust at depth of 10-20 km.

(b) A layer with high seismic P-wave velocities (7.1-7.8 km/s) is present in the crust and mantle transition zone. Its velocity increases rapidly from 6.8 km/s to 7.1-7.5 km/s from depth of 40 km to 55 km and then slowly to 7.8 km/s to depth of 60-70 km. This layer is relatively thicker in the central part of the profile than at the ends of the profile. The average thickness of this layer is 20 km with maximum of 25 km at the center of the profile. It decreases rapidly to 10 km near Lijiang (to the west) and decreases gradually to 15 km in Zhehai (to the east).

(c) There is a high-velocity, lens-shaped body (8.3-8.6 km/s) in the upper mantle at depth of 110-160 km. Surrounded by normal velocity mantle (~8.1 km/s), this high-velocity body is ~200 km long in the east-west direction and about 50 km thick. It is important to note that the location of this fast zone matches well that of the thick lower crust layer. In addition, the geometric coincidence of this high Vp body and the inner zone of the doming structure is also remarkable (Fig. 1).

Deep Seismic Reflection

Deep seismic reflection has been employed to determine the crustal thickness in the Emeishan LIP, which, together with the domal structure, is shown in Fig. 4. It is noted that there is a gradual decrease in crustal thickness from the center to the margin of the Emeishan LIP. The crustal thickness in the central part ranges from 55 to 64 km (average 61.5 km). The crust in the east part is also relatively thick, ranging 38-54 (average 45 km), but thinner than in the central part. The data beyond the Emeishan LIP are sparse but define a range of 35-45 km.

Summary

Various geophysical approaches reveal some consistent features regarding the crust-mantle structure in the Emeishan LIP. Crustal structure and crust-mantle transition in the central part of the Emeishan LIP are different from those in other areas. Specifically, three anomalously high velocity bodies (compared to their respective environs) have been detected in the upper crust (6.0-6.6 km/s), crust-mantle transition zone (7.1-7.8 km/s) and the upper mantle (8.3-8.6 km/s). All these seismically anomalous bodies are confined to the inner zone, and are generally absent or not obvious in the intermediate and outer zones (e.g., Cui et al. 1987).

The layer with velocity >7.0 km/s at the crust-mantle transition zone and underlying fast mantle (>8.3 km/s) have been observed in many LIPs, for example, the Columbia plateau (8.4 km/s, Catching and Mooney, 1988), Rhine graben (8.3-8.4 km/s, Zucca, 1984) and Ontong Java Plateau (8.6 km/s, Furumoto et al., 1990). Therefore, the crust-mantle velocity structure in the Emeishan case shares common features observed in other large igneous provinces. In next sections, we will evaluate cause(s) of crustal thickening in this region and the formation of the high velocity crust.

CRUSTAL GROWTH BY MAGMATIC UNDERPLATING DURING EMEISHAN VOLCANISM

High Velocity Layer at the Crust-Mantle Transition: Upwelling Mantle or Lower Crust?

The layer of 7.1-7.8 km/s is ubiquitously present in the crust-mantle transitional zone in the Emeishan LIP. Similar velocity has been observed in east African rift (Davis and Slack, 2002) and Baikal rift (Brazier and Nyblade, 2003) and is considered as evidence for upwelling mantle. Tan (1987) and Zhang et al. (1988) have adopted this interpretation and regarded it as evidence for upwelling asthenosphere in the Panxi (i.e., the Panzhihua-Xichang) rift zone. However, the mantle upwelling model is inconsistent with the fast upper mantle (Vp>8.3 km/s; Liu et al., 2000) rather than the low velocity mantle expected in extensional region. On the other hand, the so-called Panxi rift is Permian-Triassic in age (Zhang et al., 1988; Cong, 1988). Consequently, the upwelling mantle is not absolutely expected at the present time. Other arguments against the low velocity mantle model include thick crust along the Panxi paleo-rift, rather than the thin crust expected for the extended region. Consequently, we interpret the layer of 7.1-7.8 km/s as a part of the lower crust. In fact, high velocity lower crust (HVLC) is a characteristic of large igneous provinces (Coffin and Eldholm, 1994; Menzies et al., 2002).

Formation of the HVLC by Magmatic Underplating Associated with Emeishan Plume

Two distinct dynamic models have been proposed to explain the formation of the HVLC (see review of Kelemen and Holbrook, 1995). The plume model invokes a deep-seated thermal anomaly in upwelling mantle (White and McKenzie, 1989; Farnetani et al., 1996), whereas “secondary convection models” (Mutter et al., 1984) call upon rapid upwelling of a

mantle source without a thermal anomaly. A possible scenario in the second case is lower crustal (eclogitic?) detachment and subsequent uplift as mantle flows into the new space. However, this model encounters several problems. (a) If crustal delamination induced mantle melting which gave rise to the Emeishan flood volcanism, a thinner crust would be expected underneath the center of the Emeishan LIP. As stated in the previous section, a layer with seismic velocity 7.1-7.8 km/s is a part of the lower crust, rather than the upper mantle. Even if this high velocity layer is not taken into account, the crust beneath the inner zone is thicker than that under the intermediate zone. (b) Crustal rebound subsequent to crustal delamination would be expected to be an instantaneous effect, i.e., to occur over a short time span (a few million years). This is inconsistent with the persistant uplift which lasted for >40 Ma in the Emeishan case. (c) Fig. 4 shows a gradual decrease in crustal thickness from the center to the margin of the Emeishan LIP, with thicker crust confined to the inner zone. This spatial variation cannot be explained by the delamination model, as there is no reason to expect the delaminated crust to have a circular shape. (d) Finally, crustal delamination has not yet been physically and mechanically demonstrated. The lower crust and convective mantle are separated by buoyant subcontinental lithospheric mantle. Whether delaminated crust could penetrate the rigid lithospheric mantle is unclear.

The common practice to constrain the genesis of the HVLC is to use the geochemistry of a suite of lava samples to estimate the physical properties of the cumulates and then compare these properties with those determined by the geophysical survey (Farnetani et al., 1996; MacLennan et al., 2001), or combining modeling results and experimental data to draw the conditions under which the HVLC were formed (Kelemen and Holbrook, 1995; Trumbull et al., 2002). Both approaches require knowledge of a number of assumptions and parameters (e.g., nature of parental magmas, physical conditions under which fractionation takes place) that are not easy to determine. On the other hand, since the underplated igneous crust has never been directly sampled, it is impossible to date its formation age, leaving the geodynamic setting under which the HVLC was formed poorly constrained. The observation that the crust-mantle structure in the Emeishan LIP varies systematically in relation to the domal structure provides another insight into the origin of the HVLC.

In the Emeishan case, the HVLC is overlain by a high velocity upper crust (Vp = 6.0-6.6 km/s) and a lens-shaped, fast upper mantle (Vp = 8.1-8.6 km/s) in the upper mantle. Farnetani et al (1996) suggested that coexistence of HVLC with high upper crustal velocity is diagnostic of deep melting and HVLC layers beneath oceanic plateaus and hotspots are an integral part of plume volcanism. A similar interpretation can thus be applied in the Emeishan case. More importantly, the distribution of these seismically anomalous bodies at different levels is well within the inner zone of the Emeishan LIP. For instance, high velocity upper crust is not observed in the intermediate and outer zones. The western and eastern margins of this seismically anomalous body correspond to longitudes of 100.8°E and 102.8°E, respectively, which agree well with the geographic location of the inner zone (Xu et al., 2004). These observations are indicative of a common factor that governed the formation of these seismically anomalous bodies. As discussed by He et al. (2003), the crustal domal uplift immediately preceding eruption of the basalts most likely resulted from thermal or dynamic doming by a mantle plume that generated the Emeishan basalts. Because the domal structure and crust-mantle structure were obtained by independent methods, this correlation strongly

suggests the generation of the thick HVLC by Emeishan plume. The fast upper mantle might represent the residues left after extensive melt extraction from the plume head. Strongly refractory (olivine-rich) mantle is low in density, which translates to high compressional velocities. The high velocity upper crust and the HVLC represent intraplating and underplating of plume-derived melts at different levels of the crust.

Experiments show that primary melts derived by partial melting of mantle materials at depth are likely picritic with >16 wt% MgO. This contrasts with the predominant evolved nature (MgO < 8%) of the erupted lava. Crystal fractionation has been invoked to explain this discrepancy (Cox, 1980), because picritic magma will pond at the crust-mantle boundary due to density contrast (Sparks et al., 1980). Crystal fractionation produces cumulates, causing underplating and thickening of the crust (i.e. formation of the HVLC). According to the plume hypothesis (Campbell and Griffiths, 1990), the melt production at the central part of the plume head would be more important than at the plume head periphery, due to temperature gradient across the plume head. Another reason may be related to the uplift of mantle and crust above the plume head. The space created by lithospheric uplift will be instantaneously filled by upwelling asthenosphere/plume. This induces more decompression melting in the region above the plume head compared to the plume periphery where the lithospheric uplift is limited. To the first-order approximation, the amount of melt/cumulates trapped at the crust-mantle boundary could be proportional to the expected melt production. This explains the observed variation in crustal thickness across the doming structure of the Emeishan LIP (Fig. 4; Xu et al., 2004). This interpretation is supported by recent geochronologic studies which show the synchronism between the emplacement of mafic and ultramafic intrusions in the inner zone of the Emeishan LIP and the eruption of the Emeishan basalts. SHRIMP U-Pb zircon dating reveal that mafic and ultramafic intrusions were emplaced at 259-261 Ma (Zhou et al., 2002; Zhong et al., 2004), virtually identical to the eruption age of the Emeishan basalts inferred from the stratigraphic constraints (Courtillot et al., 1999), if a new geologic time scale (Gradstein et al., 2004) is applied.

Other supporting evidence for magmatic underplating/intraplating origin for high velocity crust comes from the sedimentary record of Late Permian to Middle Triassic (Fig. 5). Stratigraphic units below the Emeishan basalts are similar to other parts of the Yangtze craton (Zhang et al., 1988; Feng et al., 1997), indicating that this region experienced a similar geological history to other parts of Yangtze craton before the Emeishan volcanism (Fig. 5a). However, there is a dramatic change in sedimentary environment after the Emeishan volcanism in SW China (Wang et al., 1994; Xu et al., 2004). The most striking change is the appearance of an elliptical basement core (known as the Chuandian ‘old land’) in the center of the Emeishan LIP (Fig. 5b). Depositional patterns from Upper Permian to Middle Triassic suggest that crustal uplift persisted to the middle Triassic (Fig. 5c). Such a prolonged uplift (>45 Ma) may be due to magmatic underplating (White et al., 1987, 1989; McKenzie, 1984; Brodie and White, 1994), because in some instances underplating-related uplift can last for as long as > 200 Myr (Cox, 1989). It is shown in Fig. 5b that the “Chuandian old land” is surrounded by terrestrial (Xuanwei Formation) and marine clastic rocks (Longtan Formation). This sedimentologic configuration is indicative of extensive erosion of the Emeishan basalts in the inner zone, consistent with scarce Emeishan basalts in the inner zone compared to those in intermediate zone (Fig. 1). The Xuanwei clasts represent eroded products from

Emeishan basalts in the inner zone (He et al., submitted). Depositional patterns from Upper Permian to Middle Triassic show transgression, as marine clastic rocks and limestones overlapped progressively the Chuandian old land (Fig. 5d).

Possible Components in the HVLC

Before adopting a petrologic approach to constrain the composition of the HVLC based on the observed velocity values (Kelemen and Holbrook, 1995; Farnetani et al., 1996; Trumbull et al., 2002), it is important to determine (1) whether garnet plays a role in the observed high velocity layer; (2) whether this thick crust is composed of solidified liquids or of fractionated cumulate derived by crystal fractionation from an evolving liquid that later migrated upward to form the shallow crust.

Garnet has potentially important effects on the seismic crustal structure. For instance, 20% volume of garnet in a MORB-like bulk composition would increase Vp from 7.1 km/s to 7.4-7.5 km/s (Trumbull et al., 2002). This effect should be taken into account in SW China where the crust is as thick as 65 km, a condition favorable for the stability of garnet (>30 km). Nevertheless, the following considerations argue against a significant role of garnet at the base of crust of the Emeishan LIP. (a) The high velocity layer in SW China do not occur as an horizontal layer, as would be expected if the velocity of the lower crust is controlled by plagioclase-garnet phase transformation, because the latter takes place at fairly constant pressure. For instance, Vp of 7.1 km/s in the Panxi area occurs at depth of ~50 km, in contrast, similar velocity has been detected at a shallow depth (<40 km) near Lijiang. (b) The plagioclase-garnet phase transformation occurs at a depth of about 30 km. However, in SW China, velocity at this depth varies between 6.6 km/s, significantly lower than that for garnet granulites (>7.0 km/s, Rudnick, 1995). (c) As will be demonstrated later, the HVLC is likely composed of mafic-ultramafic components that have less aluminous contents than the overlying gabbros. The lack of significant amount of plagioclase may hamper the garnet-formation reaction (Farnetani et al., 1996). (d) Finally, if the HVLC is due to the presence of garnet, the high density of this material would result in mechanical instability of the mafic crust. Delamination may put fundamental limitations on the thickness of crust (~ 30 km; Sobolev and Babeyko, 1989). Trumbull et al. (2002) suggested that the crust in the Namibian margin (~130 Ma) may have lost its lower part. This clearly did not happen in SW China, although the HVLC may be much older (~ 260 Ma).

The HVLC may be composed of cumulates crystallized from picritic liquids derived by partial melting at relatively high pressure. Alternatively, the picritic melts formed some extensive and horizontal sills that crystallized as nearly closed system (Bedard et al., 1988; Dick et al., 1991). In this scenario, little crustal differentiation occurred at the site and some picritic magmas may have formed sills in the accreting lower crust, crystallizing in their entirety at depth. In the case of the Emeishan LIP, the HVLC may be predominantly composed of cumulates of pyroxene and olivine (Xu et al., 2003), although entrapment of some residual melts among cumulus minerals cannot be fully ruled out (e.g., Zhu et al., 2003). This argument is made based on the following lines. (a) The wide range of Vp of 7.1-7.8 km/s observed in SW China is not consistent with the total melt crystallization model in which no variation in seismic velocity with depth is expected. (b) As argued by Kelemen and Holbrook

(1995), the formation of sills likely occurred within 10 km of the surface where picritic magma can cool rapidly. In a thick crust (>20 km), magmas underplated at the base of crust can undergo extensive crystal fractionation as a result of slow cooling. This is the situation in SW China where the original crust thickness of about 35-40 km. (c) Solidified melts cannot account for the observed Vp as high as 7.8 km/s. As demonstrated by Farnetani et al. (1996) and later in this study, high velocity (7.8 km/s) can only be readily explained by cumulate derived by fractionation from picritic melts.

Relationship between the Emeishan Basalts and the HVLC: Petrologic Modeling

In section 4.1, a genetic link between the Emeishan basalts and the high velocity crust is established on the basis of the variation in crustal thickness across the domal structure and the synchronism between the emplacement of mafic/ultramafic intrusions and eruption of the Emeishan basalts. Here, we followed the approach of Farnetani et al. (1996) and use the observed Vp to constrain the composition of the HVLC. Low MgO (mostly <7%) and Ni contents suggest that the Emeishan basalts underwent extensive crystal fractionation from parental magmas either in magma chambers or en route to the surface (Xu et al., 2001). We assume that fractionation of picritic magma produces ultramafic cumulates (i.e., HVLC) and residual low MgO basaltic magma (Emeishan basalts). This hypothesis is apparently at odd with petrographic feature that suggests plagioclase and clinopyroxene rather than olivine as dominant fractionated minerals. Yet, the fractionation of plagioclase and clinopyroxene likely took place under relatively low pressure, whereas cumulates in the HVLC in SW China were settled at ~15 kbar.

To test this model, we used the MELTS program of Ghioso and Sack (1995) to model the compositional evolution of deep mantle plume melts, assuming that crystal fractionation is the dominant mechanism through which parental melts evolve towards basaltic magmas. The oxygen fugacity used in the calculation is the quartz-fayalite-magnetite (QFM) buffer. We used recent estimates of primary magmas (Xu and Chung, 2001) as initial melts and calculated fractionated mineral assemblage under 10 and 15 kbar. These pressures are equivalent to the thickness of the crust prior to basaltic underplating in SW China (~40 km, i.e., the crustal thickness outside of the Emeishan LIP). Plagioclase does not appear as a liquidus phases during fractionation under these pressures, consistent with the absence of Eu anomalies and increase in Al_2O_3 with decreasing MgO in the Emeishan basalts (Cong, 1988; Xu et al., 2001). Main fractionating phases include spinel (Sp), orthopyroxene (Opx), clinopyroxene (Cpx) and olivine (Ol). Orthopyroxene generally crystallizes at the beginning of fractionation, which is then dominated by Cpx. Fig. 6 shows that fractionation of picrites can produce residual melts which are compositionally similar to the Emeishan basalts. 54% fractionation of picritic melts at 15 kbar generates unltramafic cumulus with volumetric proportion of sp:cpx:opx:ol of 2.5:93.7:2.4:1.5 (Table 1). Calculated Vp for this fractionated assemblage is 7.5-7.8 km/s. A similar result is obtained for the fractionation at 10 kbar (Table 1). These calculated Vp are at high end of the observed seismic velocities (7.1-7.8 km/s) in the Emeishan LIP.

Zhu et al. (2003) argued that entrapment of a few percent of residual melts in cumulus

minerals can lower the calculated velocity to the observed values (7.1 km/s). Alternatively, the cumulate layer with lower Vp (~7.1 km/s) may be derived from a fractionating melt that lost mafic minerals in early stage of fractionation. For instance, if we chose experimental melts produced at 10 kbar (Hirose and Kushiro, 1993) as initial melts, fractionation of this melt at 10 kbar would produce an assemblage of Sp, Cpx and plagioclase with a volume proportion of 0.8:58.2:41. The corresponding Vp ranges between 7.0-7.3 km/s, which is very similar to low end of the observed seismic velocity. Another possibility to lower Vp involves the hybridization of underplated magmas with the preexisting crustal material. At this stage, it is not possible to make distinction between theses alternatives.

The high velocity (6.0-6.6 km/s) upper crust in the inner zone of the Emeishan LIP may have resulted from magmatic intraplating. To test this model, we performed calculation at lower pressures (5, 3 and 1 kbar). Because olivine becomes as liquidus phase earlier at lower pressures than at high pressure, involvement of olivine (a high velocity mineral) in fractionated assemblage (olivine gabbros) yields high velocity range at 7.6-8.0 km/s (Table 1), significantly exceeding the observed values. Even if a two-stage fractionation is considered (i.e., residual melt after fractionation at Moho depth, fractionates again at shallow crustal levels), velocity greater than 7.0 km/s is obtained for cumulates (see Farnetani et al., 1996). The observed high velocity upper crust in the Emeishan case is therefore unlikely related to mineral segregation processes of plume derived melts. It is proposed here that it may represent a mush of mineral cumulates and solidified residual melts.

IMPLICATIONS FOR THE TOTAL VOLUME OF THE EMEISHAN MAGMAS

While the mantle plume model has been increasingly adopted for the generation of the Emeishan basalts (Chung and Jahn, 1995; Xu et al., 2001), some doubts have been cast on the viability of this model because of the relatively small dimension of this igneous province compared with typical LIPs (e.g., Thompson et al., 2001). The Emeishan basalt underwent extensive erosion (Xu et al., 2004; He et al., 2006) and tectonic disruption (Xiao et al., 2003). Thus the estimates of its total volumes remain problematic. Lin (1985) estimated the average lava thickness of the Emeishan basalts to be about 700 m. Taking the exposure surface of 2.5 x 10^5 km^2, the entire volume of the Emeishan basalts is estimated to be ~0.2 x 10^6 km^3. This represents a minimum estimate (Xu et al., 2001) because: (1) complicated tectonic movements in Meso-Cenozoic eras in this region cut off the western extension of the LIP (Chung et al., 1998, Xiao et al., 2003); (2) erosion must have removed a significant portion of the eruptive sequences; and (3) the associated intrusives are not taken into account.

As discussed above, the emplacement of igneous materials in the lower crust was genetically related to the erupted basalts, therefore this high velocity layer can be considered as an integral part of the Emeishan LIP. It is possible that the HVLC occurs predominantly within the inner zone of the dome, given the contrast in the crust-mantle structure between the inner zone and other zones. In this sense, a minimum volume (2.5 x 10^6 km^3) of igneous materials accreted to preexisting crust can be estimated. A higher estimate could be expected if intraplating (i.e., magmas trapped at different crustal level) is taken into account. This estimate in turn provides constraints on the volume of the erupted lavas, as cumulates and erupted magmas can be related by mass balance (Cox, 1989):

$$C_P = C_L X_L + C_C X_C$$

Where C_P, C_L, and C_C are the concentrations of an element in parental magma, erupted liquid and cumulate respectively; X_L and X_C are the respective mass fractions of erupted liquid and cumulates. Using the above equation and elemental concentrations in parents, erupted basalts and cumulate, the ratio X_C/X_L of 0.65 is obtained. Accordingly, the minimum volume of erupted magmas is estimated to be 3.8 x 10^6 km^3, equivalent to the volume of the typical large igneous provinces on the Earth (Coffin and Eldholm, 1994). As a consequence, the volume of igneous materials is not at odd with the plume model proposed for the formation of the Emeishan LIP.

CONCLUSIONS

(1) Geophysical survey (deep seismic refraction/reflection and seismic tomography) reveals a thick and seismically heterogeneous crust beneath the Emeishan LIP. The crustal thickness decreases gradually from the inner zone (~60 km) via the intermediate zone (<45 km) to the outer zone (< 40 km). The crust in the inner zone is composed of a relatively high velocity (6.0-6.6 km/s) upper crust and a 20 km thick high velocity (7.1-7.8 km/s) lower crust. These high velocity bodies are not apparent in intermediate and outer zones. This, together with the synchronism of the emplacement of mafic/ultramafic intrusions and eruption of Emeishan basalts, strongly suggests a genetic link between the plume activity and the formation of the high velocity crust, if the crustal doming preceding the volcanism resulted from dynamic uplift induced by the plume that generated the Emeishan basalts.

(2) Considerable crustal thickening in the inner zone may have resulted from magmatic underplating associated with the Emeishan volcanism. Crustal growth by basaltic accretion to the pre-existing crust finds its supporting evidence from the systematic stratigraphic study and paleogeographic reconstruction that reveal a prolonged (~ 45 Ma) crustal elevation (i.e., the Chuandian old land) in the Emeishan LIP. The dimension of this domal permanent uplift is roughly the same as that of high-velocity lower crust detected by seismic imaging. Moreover, the extent of permanent uplift (~2 km) estimated in terms of geologic basis (He et al., 2006) suggests a 20 km thick underplated layer if the isostatic theory is applied (MacLennan and Lovell, 2002). This inferred volume of underplated materials is similar to the average thickness of the HVLC observed in the Emeishan LIP.

(3) Petrologic modeling further suggest that the HVLC is composed of cumulates (pyroxenite and olivine pyroxenites) crystallized from picritic melts. The data presented in this study therefore lend support to the conceptual model proposed by Farnetani et al. (1996) for the formation of the high velocity lower crust in large igneous provinces.

(4) The volume of the erupted lavas can be estimated since cumulates and erupted magmas can be related by mass balance (Cox, 1989). This yields a minimum volume of erupted magmas of 3.8 x 10^6 km^3, equivalent to the volume of the typical large igneous provinces on the Earth (Coffin and Eldholm, 1994).

ACKNOWLEDGEMENTS

We thank C. Farnetani and an anonymous referee for constructive reviews. Gillian

Foulger and Donna Jurdy are thanked for their editorial comments and patience. This study is jointly supported by the Natural Science Foundation of China (40421303; 40234046), the Chinese Academy of Sciences and the Guangzhou Institute of Geochemistry (GIG-CX-04-06).

References

Barton, A.J., and White, R.S., 1997. Crustal structure of the Edoras Bank continental margin and mantle thermal anomalies beneath the North Atlandtic. J. Geophys. Res., 105: 25829-25853.

Bauer, A.J., Neben, S., Schreckenberger, B., Emmermann, R., Hinz, K., Fechner, N., Gohl, K., Schulze, A., Trumbull, R.B., and Weber, K., 2000. Deep structure of the Namibia continental margin as derived from integrated geophysical studies: The MAMBA experiment. J. Geophys. Res. 105: 25829-25853.

Bedard, J.H., Sparks, R.S.J., Renner, R. Cheadle, M.J., and Hallworth, M.A., 1988. Peridotite sills and metasomatic gabbros in the eastern layered series of the Rhum complex, J. Geol. Soc. London, 145: 207-224.

Brazier, R.A., and Nyblade, A.A., 2003. Upper mantle P velocity structure beneath the Baikal Rift from modeling regional seismic data. Geophysical Res Lett 30 (4): Art. No. 1153

Brodie, J., and White, N. 1994. Sedimentary basin inversion caused by igneous underplating: Northwest European continental shelf. Geology. 22: 147-150.

Bureau of geology and mineral resources of Guizhou province (BGMRGP). 1987. Regional geology of Guizhou province. Geological Publishing House, Beijing. 698p. (in Chinese with English abstract).

Bureau of geology and mineral resources of Sichuan province (BGMRSP). 1991. Regional geology of Sichuan province. Geological Publishing House, Beijing. 745p. (in Chinese with English abstract).

Campbell, I.H., and Griffiths, R.W., 1990. Implications of mantle plume structure for the evolution of flood basalts. Earth Planet. Sci. Lett. 99:79-93.

Caress, D.V., McNutt, M.K., Detrick, R.S. and Mutter, J.C., 1995. Seismic imaging of hotspot-related crustal underplating beneath the Marquesas Islands, Nature, 373, 600-603.

Catchings, R.D., and W.D. Mooney, 1988. Crustal structure of the Columbia Plateau: evidence for continental rifting, J. Geophys. Res. 93: 459-474.

Chung, S.L., and Jahn, B.M. 1995. Plume-lithosphere interaction in generation of the Emeishan flood basalts at the Permian-Triassic boundary. Geology. 23: 889~892.

Chung, S.L., Jahn, B.M., Wu, G.Y., Lo, C.H., and Cong, B.L., 1998. The Emeishan flood basalt in SW China: a mantle plume initiation model and its connection with continental break-up and mass extinction at the Permian-Triassic boundary. In: Flower, M.F.J., Chung, S.L., Lo, C.H. and Lee, T.Y. (eds.), Mantle Dynamics and Plate Interaction in East Asia. AGU Geodyn. Ser., 27: 47-58.

Chung, S.L., Lee, T.Y., Lo, C.H., Wang, P.L., Chen, C.Y., Nguyen, T.Y., Tran, T.H., and Wu, G.Y., 1997. Intraplate extension prior to continental extrusion along the Ailao Shan-Red River shear zone. Geology, 25: 311-314.

Coffin, M.F., and Eldholm, O., 1994. Large igneous provinces: Crustal structure, dimension, and external consequences. Rev. Geophys., 32: 1-36.

Cong, B., 1988. The formation and evolution of the Panxi paleo-rift system. Scientific publishing house (in Chinese).

Courtillot, V.E., Jaupart, C., Manighetti, I., Tapponnier, P., and Besse, J., 1999. On causal links between flood basalts and continental breakup, Earth Planet. Sci. Lett. 166: 177-195.

Cox, K.G., 1980, A model for flood basalt volcanism, J. Petrol. 21, 629-650.

Cox, K.G. 1989. The role of mantle plumes in the development of continental drainage patterns. Nature. 342: 873-877.

Cox, K.G. 1993, Continental magmatic underplating, Royal society of London Philosophical Transactions, ser. A. 342,155-166.

Cui, Z.Z., Luo, D.Y., Chen, J.P., Zhang, Z.Y., and Huang, L.Y., 1987. Deep crust structure and tectonics in the Panxi area.

Acta Geophysica Sinica, 30: 566-579

Davis, P.M., and Slack, P.D., 2002. The uppermost mantle beneath the Kenya dome and relation to melting, rifting and uplift in East Africa**.** Geophyical Research Letters 29 (7): Art. No. 1117.

Dick, H.J.B., Meyer, P.S., Bloomer, S., Kirby, S., Stakes, D., and Mawer C., 1991. Lithostratigraphic evolution of an in-situ section of oceanic layer 3. Proc. Ocean Drill Program Sci results, 118: 439-538.

Farnetani, C.G., and Richards, M.A., 1996). Numerical investigation of the mantle plume initiation model for flood basalt event. J. Geophy. Res, 99: 13813-13883.

Farnetani, C.G., Richards, M.A., Ghiorso, M.S., 1996. Petrological models of magma evolution and deep crustal structure beneath hotspots and flood basalts. Earth Planet. Sci. Lett., 143: 81-94.

Feng, Z.Z., Yang, Y.Q., and Jin, Z.K, 1997. Lithofacies paleography of Permian of south China. Petroleum University Press, Beijing. 242p. (in Chinese with English abstract).

Furlong, K.P., and Fountain, D.M., 1986. Continental crustal underplating: thermalconsiderations and seismic-petrological consequence. J Geophys. Res 91: 8285-8294

Furumoto, A,S, Webb, J.P., Odegard, M.E., and Husong, D.M., 1976. Seismic studies on the Ontong lava Plateau, Tectonophysics 34: 71-90.

Ghioso, M.S., and Sack, R.O., 1995. Chemical mass transfer in magmatic processes, IV. A revised and internally consistent thermodynamic model for the interpretation and extrapolation of liquid-solid equilibria in magmatic systems at elevated temperatures and pressure. Contrib. Mineral. Petrol., 119: 197-212

Gradstein, F.M., Ogg, J.G., Smith, A.G., Bleeker, W. and Lourens, L.J., 2004. A new geologic time scale, with special reference to Precambrian and Neogene. Episodes 27, 83-100.

Hanski, E., Walker, R.J., Huhma, H., Polyakov, G.V., Balykin, Hoa T.T., and Phuong, N.T., 2004. Origin of the Permian-Triassic komatiites, northwestern Vietnam. Contrib. Mineral. Petrol. 147: 453-469

He, B., Xu, Y.G.., Chung, S.L., Xiao, L., and Wang, Y.M. 2003. Sedimentary evidence for a rapid, kilometer scale crustal doming prior to the eruption of the Emeishan flood basalts. Earth Planet. Sci. Lett. 213:391-405.

He, B., Xu, Y.G., Wang , Y.-M., Luo, Z.Y., 2006. Sedimentation and lithofacies paleogeography in SW China before and after the Emeishan flood volcanism: New insights into surface response to mantle plume activity. Journal of Geology 114: 117-132

Hirose, K., and Kushiro, I., 1993. Partial melting of dry peridotites at high pressure: determination of compositions of melts segregated from peridotite using aggregates of diamond. Earth Planet. Sci. Lett., 114: 477-489.

Kelemen, P., and Holbrook, S., 1995. Origin of thick, high-velocity igneous crust along the U. S. East Coast margin. J. Geophy. Res., 100, 10077-10094.

Lin, J.Y., 1985. Spatial and temporal distribution of Emeishan basaltic rocks in three southwestern province (Sichuan, Yunnan and Guizhou) of China. Chinese Sci. Bull., 12: 929-932 (in Chinese)

Liu, J., Liu, F., He, J., Chen H., and You, Q., 2001. Study of seismic tomography in Panxi palerift area of southwestern China – structural features of crust and mantle and their evolution. Science in China, (Series D), 44, 277-288.

Liu, Y.L., Wu, C.Z., Chen, J.C., Liu, H.C., Wu, L.G., and Li, S.Y., 1987. Gravity anomaly features of Dukou-Xizang area and a study of rift problems. In Yuan XC (ed) Contribution to the Panzhihua-Xichang Rift, China, III. Geological Publishing House, Beijing. 90-98. Geological Press (in Chinese).

Liu, F.T., Liu, J.H,, Zhong, D.L., He, J.K., Yu, Q., 2000. The subducted slab of Yangtze continental block beneath the Tethyan orogen in western Yunnan. Chinese Sci. Bull. 45: 466

MacLennan, J., and Lovell, B. 2002. Control of regional sea level by surface uplift and subsidence caused by magmatic underplating of Earth's crust. Geology. 30: 675-678.

MacLennan, J., McKenzie, D., Gronvold, K. and Slater, L., 2001. Crustal accretion under northern Iceland. Earth Planet Sci Lett., 191: 295-310

Menzies, M.A., Klemperer, S.L., Ebinger, C.J., and Baker, J. 2002. Characteristics of volcanic rifted margins. In "Volcanic

Rifted Margins", M.A. Menzies, S.L., Klemperer, C.J. Ebinger, J. Baker, eds., Geological Society of America Special Paper 362, 1-14.

Mutter, J.C., Talwani, M., and Stoff,a P.L., 1984. Evidence for a thick oceanic crust adjacent to the Norwegian margin. J. Geophys. Res., 89: 483-502.

Mauffret, A., and Leroy, S., 1997. Seismic stratigraphy and structure of the Caribbean igneous province. Tectonophysics, 283: 61-104.

McKenzie, D. 1984. A possible mechanism for epeirogenic uplift. Nature. 307: 616-618

Rudnick, R.L., 1995. Making continental crust. Nature, 278: 571-578.

Rudnick, R.L., and Jackson, I. (1995) Measured and calculated elastic wave speeds in partially equilibrated mafic granulite xenoliths: Implications for the properties of an underplated lower continental crust. J. Geophys. Res, 100, 10211-10218.

Saunders, A.D., Jones, S.M., Morgan, L.A., Pierce, K.L., Widdowson, M., and Xu, Y.G., 2006. The role of mantle plumes in the formation of continental large igneous provinces: field evidence used to constrain the effects of regional uplift. Chemical Geology, in press

Sheth, H., 2006. Plume-related regional pre-volcanic uplift in the Deccan Traps: Absence of evidence, evidence of absence. Geological Society of America Special Paper ###, p. 000-000 (this volume).

Sobolev, S.V., and Babeyko, A.Y., 1989. Phase transformations in the lower continental crust and its seismic structure. In: Mereu, R.S., Muller, S., and Fountain, D.M. (eds), Properties and processes of Earth's lower crust: AGU Geophysical Monograph, 51: 311-320

Sparks, R.S.J., Meyer, P., and Sigurdsson, H., 1980. Density variation amongst mid-ocean ridge basalts: implications for magma mixing and the scarcity of primitive lava. Earth Planet. Sci. Lett., 46, 419-430

Sun, R, Liu F, and Liu J, 1991, Seismic tomography of Sichuan. Acta Geophysica Sinica, 34: 708-716.

Tan, T.K., 1987. Geodynamics and tectonic evolution of the Panxi rift. Tectonophysics, 133: 287-304.

Teng, W.J., 1994. Physics and dynamics of the lithosphere in the Kangdian tectonic belt. Scientific Press. 256p (in Chinese)

Thompson, G.M., Ali, J.R., Song X., and Jolley D.W., 2001. Emeishan basalts, SW China: reappraisal of the formation's type area stratigraphy and a discussion of its significance as a large igneous province. J. Geol. Soc., 158: 593-599.

Trumbull, R.B., Sobolev, S.V., and Bauer, K. 2002. Petrophysical modeling of high seismic velocity crust at the Namibian volcanic margin. In "Volcanic Rifted Margins", M.A. Menzies, S.L., Klemperer, C.J. Ebinger, J. Baker, eds., Geological Society of America Special Paper, 362, 225-234.

Wang, L.T., Lu, Y.B., Zhao, S.J., and Luo, J.H. 1994. Permian lithofacies paleogeography and mineralization in south China, Geological Publishing House, Beijing, 147p. (in Chinese with English abstract).

Watts, A.B., and U.S. ten Brink, 1989. Crustal structure, flexure and subsidence history of the Hawaiian Islands, J. Geophys. Res, 94, 10473-10500.

White R., and McKenzie, D., 1989. Magmatism at rift zones: the generation of volcanic continental margins and flood basalts. J. Geophys. Res., 94: 7685-7729.

White, R., and D. McKenzie, 1995. Mantle plumes and flood basalts, Journal of Geophysical Research, 100: 17543-17585.

Yan, Q., Zhang, G., Kan, R., and Hu, H., 1985, The crust structure of Simao to Malong profile, Yunnan Province, China. Journal of Seismological research, 8(2): 249-280.

Xiao, L., Xu, Y.-G., Chung, S.-L., B. He, and Mei, H.J., Chemostratigraphic Correlation of Upper Permian Lava Succession from Yunnan Provinc, China: Extent of the Emeishan Large Igneous Province. International Geologic Review, 45: 753-766

Xiong, S., Teng, J., Yin, Z., Lai, M., and Huang, Y., 1986. Explosion seismological study of the structure of the upper mantle at the southern part of the Panxi tectonic belt. Acta Geophyscia Sinica, 29: 235-244.

Xu, Y.G., and Chung, S.L., 2001. The Emeishan large igneous province: Evidence for mantle plume activity and melting conditions. Geochimica, 30: 1-9

Xu, Y.G., Chung, S.L., Jahn B.M., Wu, G.Y. 2001. Petrologic and geochemical constraints on the petrogenesis of Permian-Triassic Emeishan flood basalts in southwestern China. Lithos. 58: 145-168.

Xu, Y.G., Mei, H.J., Xu, J.F., Huang, X.L., Wang, Y.J., and Chung, S.L. 2003. Origins of two differentiation trends in the Emeishan flood basalts. Chin. Sci. Bull. 48: 390-394.

Xu, Y.G, He, B, Chung, S.L, Menzies, M.A., and Frey, F.A. 2004. The geologic, geochemical and geophysical consequences of plume involvement in the Emeishan flood basalt province. Geology 30(10): 917-920.

Yuan, X.C., 1995, Geophysical maps of China. Geological Publishing House, Beijing, 200p.

Zhang, Y.X., Luo, Y.N., and Yang, Z.X. 1988. Panxi Rift. Geological Publishing House, Beijing. 466p. (in Chinese with English abstract).

Zhang, Y.G., and Ma, D.B., 1985. The investigation of seismic wave velocity and crustal structure in Sichuan region by use of mine explosions. Acta Geophysica Sinica, 28 (4) 377-388 (in Chinese with English abstract).

Zhong, H., Yao, H., Prevec, S.A. 2004. Trace-element and Sr-Nd isotopic geochemistry of the PGE-bearing Xinjie layered intrusion in SW China. Chem. Geol. 203: 237-252

Zhou, M., Malpas, J., Song, X., Robinson, P.T., Sun, M., Kennedy, A.K., Lesher, C.M., and Keays, R.R., 2002, A temporal link between the Emeishan large igneous province (SW China) and the end-Guadalupian mass extinction: Earth Planet. Sci. Lett., 196: 113–122.

Zhou, M.F., Robinson, P.T., Lesher, C.M., Keays, R.R., Zhang, C.J., and Malpas, J., 2005. Geochemistry, petrogenesis and metallogenesis of the Panzhihua gabbroic layered intrusion and associated Fe-Ti-V oxide deposits, Sichuan Province, SW China. J Petrol., 46: 2253-2280

Zhu, D., Luo, T.Y., Gao, Z.M., and Zhu, C.M. 2003. Differentiation of Emeishan flood basalts at the base of the crust and throughout the Crust of Southwest China. International Geology Review. 45: 471-477

Zucca, J.J., 1984. The crustal structure of the southern Rhinegraben from re-interpretation of seismic refraction data. J. Geophys. 55: 13-22.

Figure caption

Fig. 1 Map showing geology of the Emeishan large igneous province and distribution of geophysical experiments. Dashed circular curves separate the inner, intermediate and the outer zones, which are defined in terms of erosion extent of the Maokou Formation (He et al., 2003). The dash-dotted lines (A-A', B-B', C-C' and D-D') indicate the profile along which seismic sounding results shown in Fig. 2. Solid lines labeled with F indicate faults: F_1 - Longmenshan thrust fault; F_2 - Ailaoshan-Red River fault; F_3 - Xiaojiang fault; F_4 - Xichang-Qiaojia fault; F_5-Jinhe fault.

Fig. 2 Seismic sounding profiles (modified after Xiong et al., 1986; Cui et al., 1987; Yan et al., 1986; Tan, 1987; Teng, 1994). Location of the profiles (line A-A'; B-B'; C-C' and D-D') is shown in Fig. 1.

Fig. 3 Seismic tomographic velocity structure of the crust and upper mantle beneath west Yangtze craton (modified after Liu et al., 2001). Location of the seismic profile from Lijiang to Zhehai (line A-A') is shown in Fig. 1. HVLC—high-velocity lower crust.

Fig. 4 Crustal thickness data plotted over domal area of Emeishan large igneous province. Data sources: Zhang et al. (1988); Yuan (1995).

Fig. 5 Diagram showing changes in sedimentation and lightfaces paleogeography before and after the Emeishan volcanism. (a) A stable, homogeneous carbonate platform in the Maokou stage, which is much bigger than the Emeishan LIP. The isopach contours of remnant Maokou Formation indicates a domal thinning; (b) Paleogeography in the Wujiapingian; (c) lithofacies paleogeography in the Middle Triassic. (d) A cross section along the profile E-E' (see (c) for location of the profile). Numbers indicate thickness in meters. Data compiled from Feng et al. (1997); Wang et al. (1994); BGMRGP (1978); BGMRSP (1991). Modified after He et al. (2006)

Fig. 6 Variation of selected major oxides against MgO for the Emeishan basalts in the inner zone (Xu et al., 2003 and unpublished data). Also shown are fractionation trends at 1 kbar and 15 kbar, calculated using MELTS by Ghioso and Sack (1995). The composition of the primary melt is after Xu and Chung (2001).

Table 1 Calculation results of fractionation at different pressures

	SiO_2	TiO_2	Al_2O_3	FeO	MgO	CaO	Na_2O	K_2O	Proportion of fractionated minerals				F	Calculated Vp
									Sp	Cpx	Opx	Ol		
Parental melt	44.75	2.55	7.27	12.50	16.77	12.78	1.31	0.19						
Residual melt														
15 Kbar	39.98	4.53	9.56	17.23	13.01	11.1	2.41	0.40	2.5	93.7	2.4	1.5	54.0	7.5-7.8 km/s
10 Kbar	41.01	4.86	10.89	16.44	10.59	10.45	2.72		2.0	77.3	8.5	12.1	59.0	7.5-7.8 km/s
5 Kbar	43.13	4.67	11.58	14.40	9.35	10.92	2.70	0.89	2.5	70.3	0.0	27.2	56.3	7.6-7.9 km/s
3 Kbar	44.05	4.45	11.5	13.49	9.2	11.52	2.56	0.82	2.4	58.6	0.0	39.0	52.4	7.6-8.0 km/s
1 Kbar	44.76	4.22	11.23	12.8	9.3	12.3	2.40	0.36	2.5	53.0	0.0	44.5	48.2	7.8-8.0 km/s

Note: Calculation is performed using petrologic code MELTS (Ghiorso and Sack, 1995); Composition of parental magams is from Xu and Chung (2001).

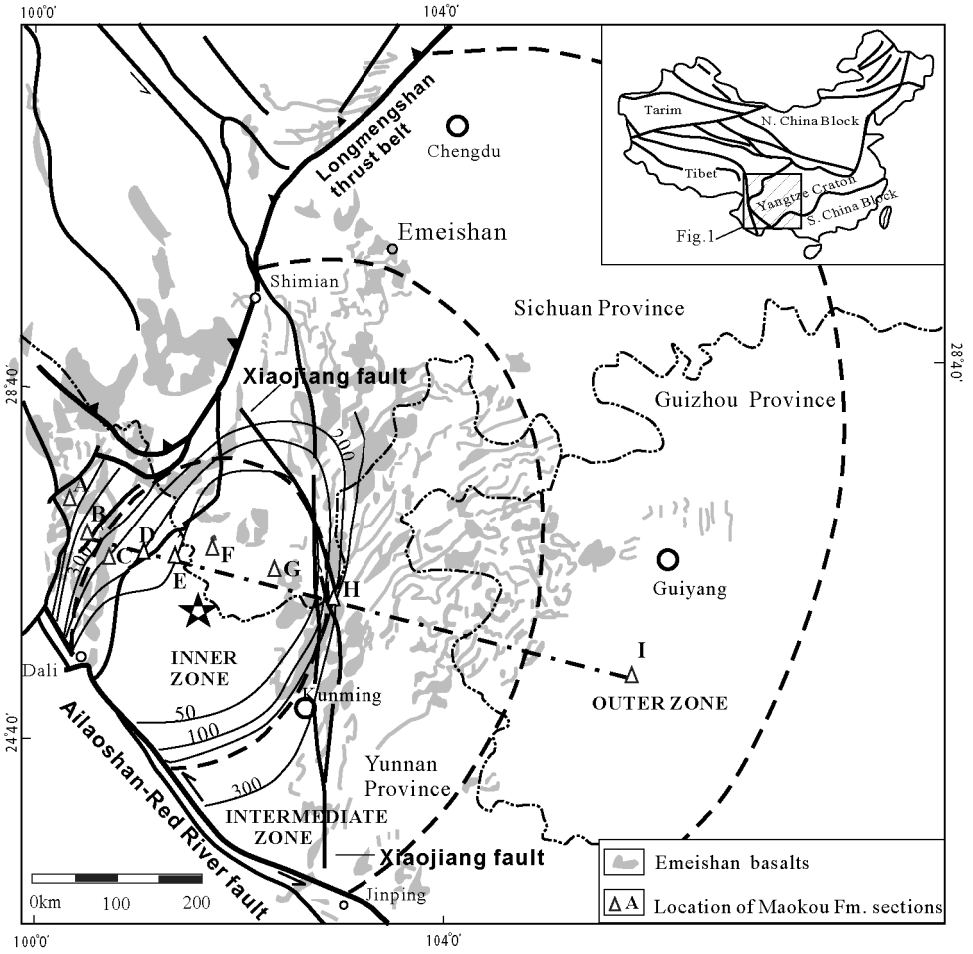
100°0'
104°0'
28°40'
24°40'
Longmengshan thrust belt
Chengdu
Emeishan
Shimian
Sichuan Province
Xiaojiang fault
Guizhou Province
200
300
A
B
C
D
E
F
G
H
I
Guiyang
INNER ZONE
Dali
Kunming
OUTER ZONE
50
100
300
Ailaoshan-Red River fault
Yunnan Province
INTERMEDIATE ZONE
Xiaojiang fault
Jinping
0km
100
200
Emeishan basalts
Location of Maokou Fm. sections
Tarim
N. China Block
Tibet
Yangtze Craton
S. China Block
Fig.1

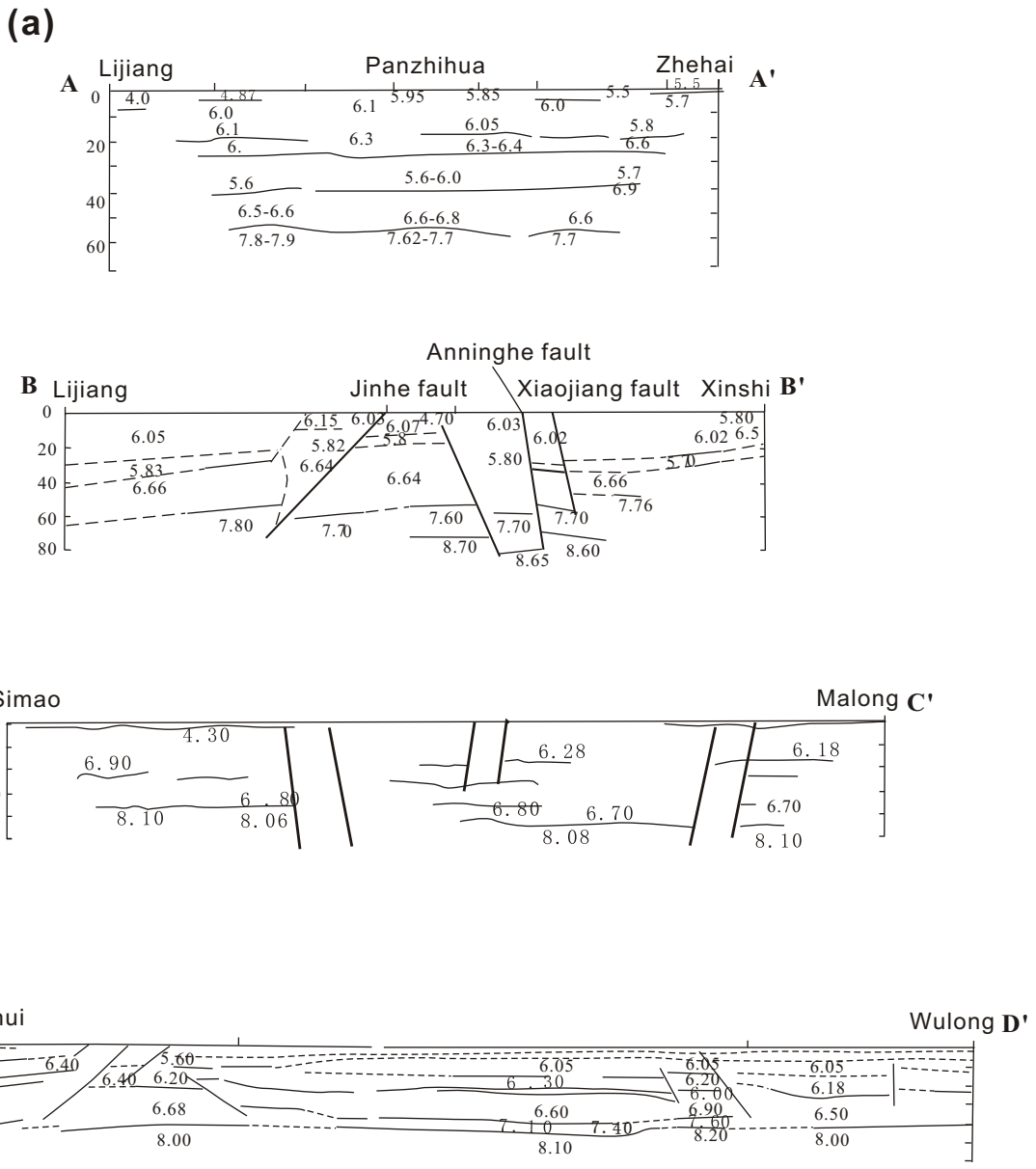
(a)
A
Lijiang
Panzhihua
Zhehai
A'
(b)
B
Lijiang
Anninghe fault
Jinhe fault
Xiaojiang fault
Xinshi
B'
(c)
C
Simao
Malong
C'
(d)
D
Heishui
Wulong
D'

Fig.2

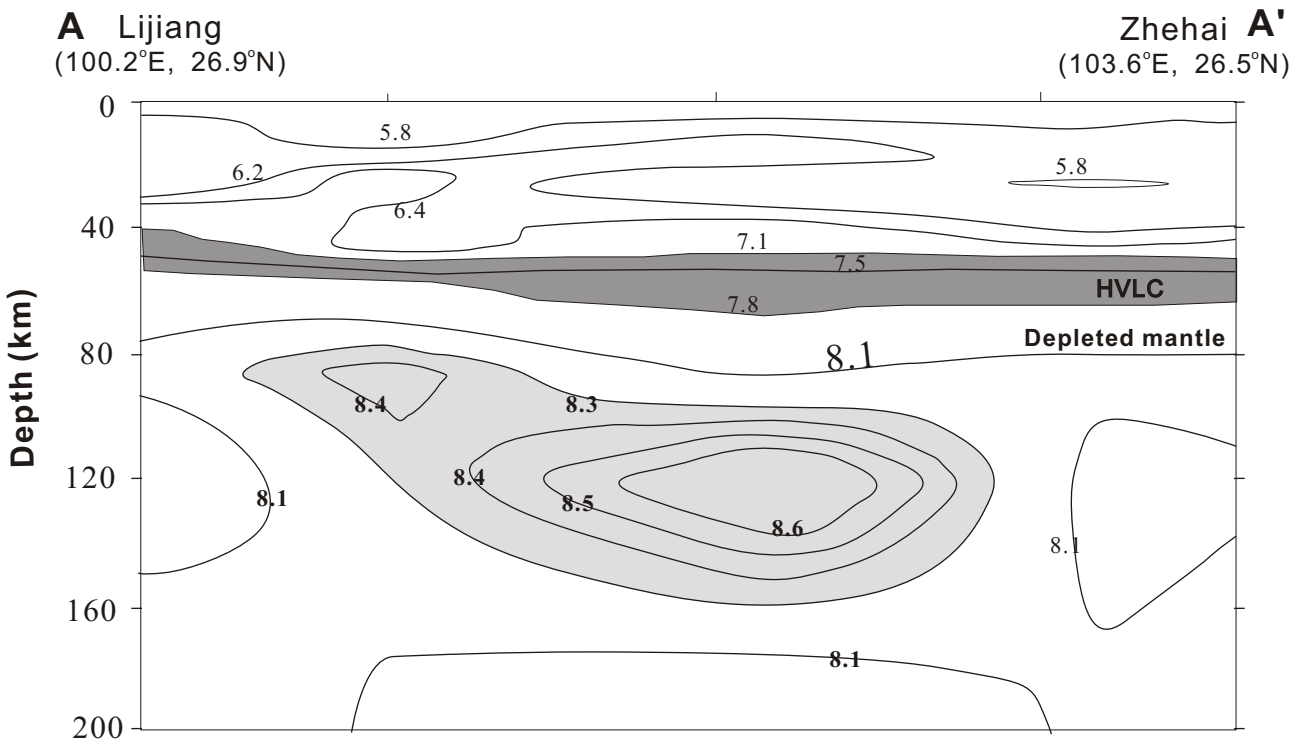
A Lijiang
(100.2°E, 26.9°N)
Zhehai A'
(103.6°E, 26.5°N)
Depth (km)
0
40
80
120
160
200
5.8
6.2
6.4
5.8
7.1
7.5
7.8
HVLC
Depleted mantle
8.1
8.4
8.3
8.4
8.5
8.6
8.1
8.1
8.1

Fig.3

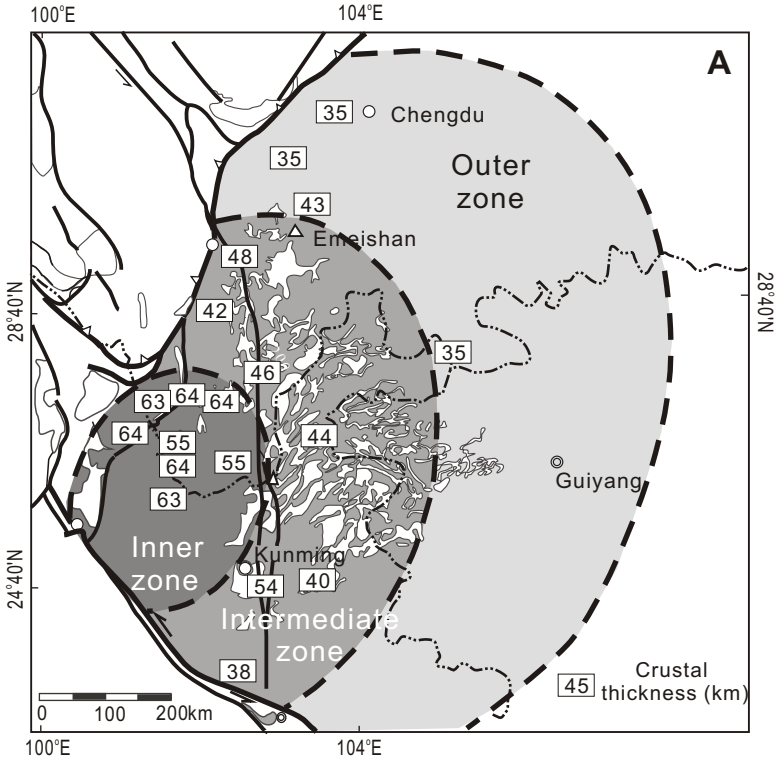
100°E
104°E
A
35
Chengdu
35
Outer
zone
43
Emeishan
48
42
28°40'N
28°40'N
35
46
63
64
64
64
55
64
55
44
63
Guiyang
Inner
zone
Kunming
54
40
Intermediate
zone
38
45
Crustal
thickness (km)
0
100
200km
24°40'N
100°E
104°E

Fig.4

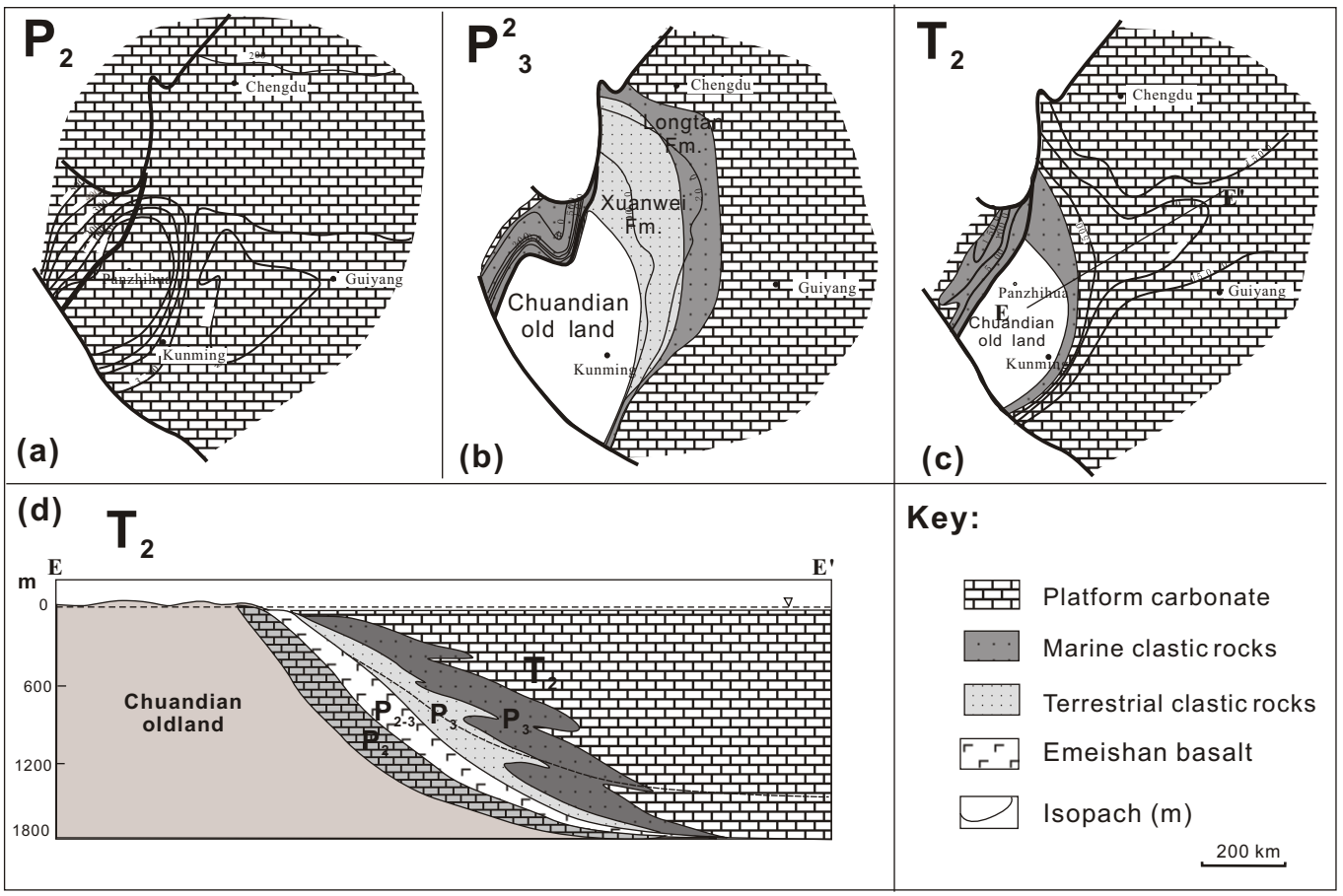
P2
Chengdu
Panzhihua
Guiyang
Kunming
(a)
P2 3
Chengdu
Longtan Fm.
Xuanwei Fm.
Chuandian old land
Guiyang
Kunming
(b)
T2
Chengdu
E
Panzhihua
Guiyang
E
Chuandian old land
Kunming
(c)
(d)
T2
m
E
E'
0
600
1200
1800
Chuandian oldland
T1
P2-3
P3
P3
P2
Key:
Platform carbonate
Marine clastic rocks
Terrestrial clastic rocks
Emeishan basalt
Isopach (m)
200 km

Fig.5

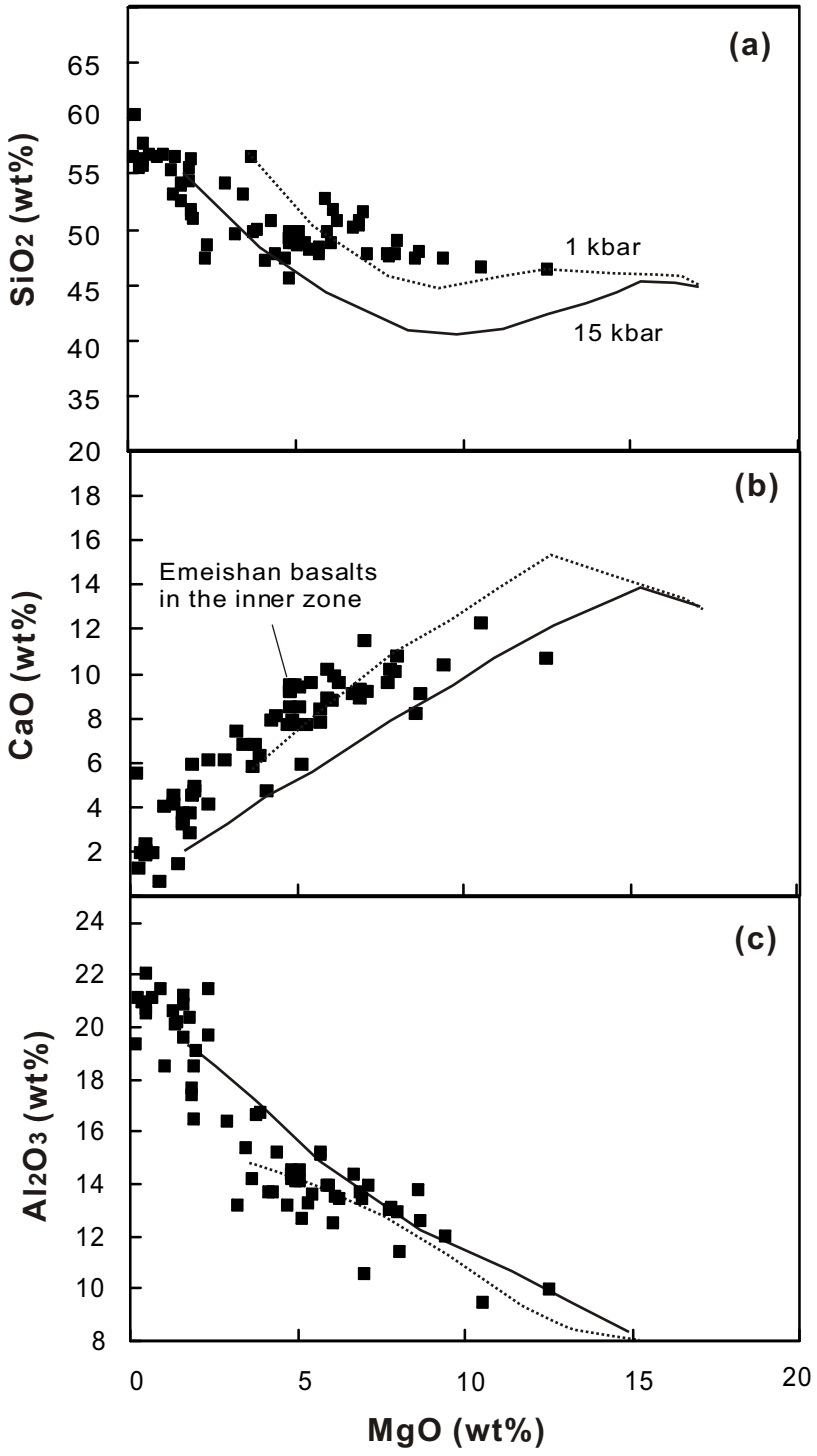
(a)
SiO2 (wt%)
65
60
55
50
45
40
35
20
1 kbar
15 kbar
(b)
CaO (wt%)
18
16
14
12
10
8
6
4
2
Emeishan basalts
in the inner zone
(c)
Al2O3 (wt%)
24
22
20
18
16
14
12
10
8
0
5
10
15
20
MgO (wt%)